Proceedings of the 17th International Symposium on the Packaging and Transportation of Radioactive Materials
PATRAM 2013
August 18-23, 2013, San Francisco, CA, USA

ESTABLISHMENT OF NEW CONSEQUENCE ASSESSMENT SYSTEM FOR EMERGENCY RESPONSE OF COMPETENT AUTHORITY TO MARITIME TRANSPORT ACCIDENTS INVOLVING RADIOACTIVE MATERIAL

Mitsufumi ASAMI
National Maritime Research Institute
Hideyuki OKA
National Maritime Research Institute
Ken-ichi SAWADA
National Maritime Research Institute
Yoshihiro HIRAO
National Maritime Research Institute
Seiki OHNISHI
National Maritime Research Institute
Hiromitsu MOCHIDUKI
National Maritime Research Institute
Akiko KONNAI
National Maritime Research Institute
Naoteru ODANO
National Maritime Research Institute

ABSTRACT

National Maritime Research Institute has developed and maintained a supporting system for emergency response of competent authority to maritime transport accidents involving radioactive material since 2005. The supporting system for emergency response has functions of air diffusion simulation, marine diffusion simulation and radiological impact evaluation to grasp potential hazard of radioactive material caused by the falling to the ocean of the package or by the collision with other vessels. In response to this situation, the urgent need for the configuration of the new supporting system was recognized. The new supporting system contains functions as follows; the diffusion calculation of radioactive material can be performed not only in the open ocean but in local area around port and harbor for the sake of the employee and public to expose radiation which is as low as reasonably achievable. In order to prevent employee, who contributes to accident mitigation, from radiation exposure, it is necessary for the supporting system to calculate the current of air and in the ocean by practical forecast data including meteorological characteristics and sea states. In the supporting system, the diffusion calculation for radioactive material is performed by Lagrange model with consideration for current of air and in the ocean. The use of this model enables calculation in a short time which responds to emergency action. Additionally, the graphical user interface of the supporting system is enhanced to make it possible to evaluate rapidly the result which is obtained by the supporting system. This paper shows the principal improving point and the concrete method of utilization of the supporting system.

INTRODUCTION

National Maritime Research Institute has developed a supporting system for emergency response of competent authority to maritime transport accidents involving radioactive material as a part of nuclear emergency preparedness in the wake of a serious Tokai-mura criticality accident which occurred on 30 September 1999.

The development of a system for the environmental assessment of transport accidents involving radioactive material starts after the enactment of National Environmental Policy Act (NEPA) of 1969[1] and under contract to the Nuclear Regulatory Commission (NRC), as an analytical tool during preparation of the “Final Environmental Statement on the Transportation of Radioactive Material by Air and Other Modes".[2] In 1979, the RADTRAN code was developed by Sandia National Laboratories.[3] After that, in 1983, International Atomic Energy Agency (IAEA) developed INTERTRAN code which was a globalized version of the RAMTRANS code.[4] These systems include the Gaussian plume model which is the most widely used method of estimating downwind concentrations of air borne material released to the atmosphere.[5, 6, 7] When the environmental assessment of hypothetical accident is performed for the purpose of preliminary survey, the Gaussian plume model is commonly used for the accidental release of radio-nuclides to the atmosphere. In meteorological guide for safety analysis of nuclear power reactor facilities (Decision by the Nuclear Safety Commission, Japan), the Gaussian plume model is used for the dose assessment under normal and accident release conditions. Based on the guide, National Maritime Research Institute developed the system for environmental assessment by using the Gaussian plume model in 2004.

The Gaussian plume model has several inherent limitations as follows: the model is based on the assumption of homogeneous turbulence in the atmosphere which makes the diffusion coefficients independent of position. Horizontal homogeneity is approached if the terrain is flat and uniform. Vertical homogeneity is harder to achieve since the wind speed tends to increase with elevation, thereby, altering the vertical distribution of turbulent eddies. The constant wind speed condition allows all parts of the plume to move advectively with the same speed. The Gaussian plume model requires that air concentrations be averaged over a sufficiently long time interval so as to smooth out spatial fluctuation in the plume.

For the actual emergency response measure to evacuate general public, it is necessary to be the numerical model which can take into account the feature of the air diffusion on complicated geographical feature and the weather change according to time and space. In the current supporting system, we can predict the dispersion of radioactive materials in three-dimension, time dependent wind and turbulence fields. The atmospheric dispersion model in the supporting system allows assessment of the impact of one or multiple sources emitted into complex local weather regimes including complex terrain. Daily operational weather forecasting data, which is called Grid Point Values (GPV), provided by Japan Meteorological Agency, can be used for the supporting system.

On the other hand, in Japan, most of nuclear fuel materials used at nuclear power plants are transported by general cargo ships from abroad while spent fuels are transported to nuclear fuel reprocessing plants by shipping vessels in exclusive use. Although the spent nuclear fuel had been transported to a reprocessing plants in UK and France from each nuclear power station by exclusive shipping vessels, sea transport of spent fuels from each nuclear power station to domestic reprocessing plants took lead because receipt of spent nuclear fuel at a storage facility in the reprocessing plant of Japan Nuclear Fuel Ltd. (JNFL) located at Rokkasyo-mura has been started since 1998. The low level radioactive wastes (LLW) have been transported to the LLW burial site of JNFL located at Rokkasyo-mura. As described above, it is important for Japan to transport radioactive materials by ship. In foreign countries other than Japan, radioactive materials are transported mainly by land. This is the reason why the environmental assessment system is considered only in rail and road transportation. Therefore, the general-purpose environmental assessment system to sea transport of radioactive material recognized internationally does not exist. In Japan, dose assessment for general public by packages shipping various radioactive materials hypothetically sunk into the sea was carried out for the public acceptance of safe transport of radioactive materials through case studies developing assessment

methods.[8, 9, 10, 11, 12] In recent years, distribution of oceanic ^{137}Cs emitted from the Fukushima Daiichi Nuclear Power Plant was simulated numerically by a regional ocean model system (ROMS) with which a highly precise result is obtained.[13] In the current supporting system, the ocean dispersion simulation code can assess nuclide concentration distributions in ocean due to release of radioactive materials from the sunken package. The ocean dispersion model for detailed evaluation is based on three-dimensional diffusion equation in consideration of nuclides decay and scavenging. The simulation code can assess effective dose due to external and internal exposure. The dispersion model can apply for all costal region of Japan no matter where radioactive packages are transported. Ocean flow data, which is called Japan Coastal Ocean Predictability (JCOPE) Experiment data,[14] provided by Japan Oceanographic Data Center can be used for the supporting system.

OVERVIEW OF THE SUPPORTING SYSTEM FOR EMERGENCY RESPONSE TO MARITIME TRANSPORT ACCIDENTS INVOLVING RADIOACTIVE MATERIAL

The supporting system for emergency response is composed of atmospheric dispersion simulation code, ocean dispersion simulation code and radiation shielding calculation code and database as shown in **Figure 1**.

Daily operational weather forecasting data, which is called Grid Point Values (GPV), provided by the Japan Meteorological Agency (JMA), is used for the atmospheric dispersion simulation. In order to obtain a current of air, we interpolate the GPV between coarse grids by using the mass-consistent flow simulation (MASCON) model.[15, 16] Calculus of finite differences is used for numerical analysis. The atmospheric dispersion simulation code can assess nuclide concentration distributions in air due to release of radioactive materials from the package(s). Staggered grid is used for computational grid, which has the advantage of superior computational stability.

Ocean flow data, which is called Japan Coastal Ocean Predictability (JCOPE) Experiment data, provided by Japan Oceanographic Data Center can be used for the supporting system. The JCOPE data in the supporting system has been updated automatically each time the data delivered and reanalysis data which is the data averaged over given period of time has been calculated. Then these data is stored external disk storage system. The supporting system has JODC-Expert Grid data for Geography (J-EGG500) which is a 500m gridded bathymetric dataset provided by Japan Oceanographic Data Center, JODC; A huge amount of the depth-sounding survey data around Japan have been integrated and gridded by 500m intervals to be used for general purposes. In order to obtain a current in the ocean, we interpolate the JCOPE data and reanalysis data between coarse grids by using the mass-consistent flow simulation (MASCON) model. Calculus of finite differences is used for numerical analysis. The ocean dispersion simulation code can assess nuclide concentration distribution in ocean due to release of radioactive materials from the sunken package(s). Staggered grid is used for computational grid, which has the advantage of superior computational stability.

The calculation model used for these dispersion simulation codes is based on Lagrangian particle transport model which was designed for calculating the long-range and mesoscale dispersion of nuclide concentration in air/sea from point sources. Lagrangian particle models compute trajectories of a large number of so-called particles (not necessarily representing real particles, but infinitesimally small air parcels) to describe the transport and diffusion of tracers in the atmosphere. The main advantage of Langrangian models is that, unlike in Eulerian models, there is no numerical instantaneously mixed within a grid box, whereas Lagrangian models are independent of a computational grid and have, inprinciple, infinitesimally small resolution.

The radiation shielding calculation code can assess dose distribution inboard the shipping vessels both at normal condition and at accident condition by means of Monte Carlo simulation method.

The assessed radioactive contents are spent fuel (SF), high level wastes (HLW), fresh mixed oxide, fresh uranium fuel, UO_2 powder, natural uranium hexafluoride (UF_6), enriched uranium hexafluoride and low level wastes (LLW). These are main packages in Japanese maritime transport. Shielding calculation models for the exclusive shipping vessels, container vessels and normal cargo vessels were prepared.

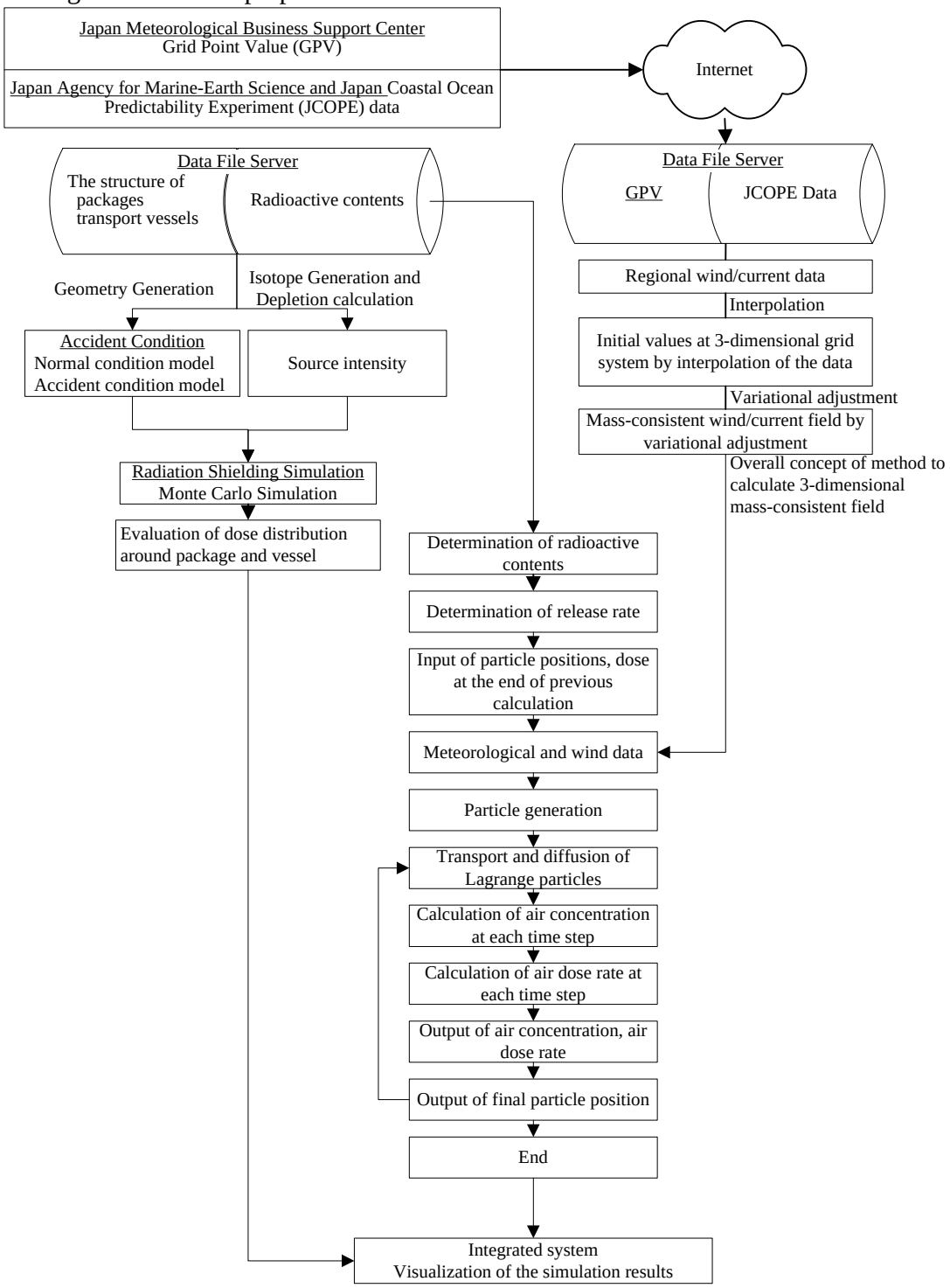

Figure 1. Overview of the supporting system for emergency response to maritime transport accidents involving radioactive material

Integrated system has a function of visualization of the simulation results and databases. The databases consist of input data set for accident assessment such as nuclide composition of each transport packages as well as information on transport packages and transport vessels.
In the present study, the discussion to the supporting system was limited to the atmospheric dispersion simulation code and ocean dispersion simulation code. For radiation shielding calculation code and database, we discussed the previous paper. [24]

Determination of first order of estimate value at the grid point on a fine mesh

Meteorological variables such as atmospheric data are routinely collected around the world but observation sites are located rather randomly from a spatial perspective. On the other hand, most computer forecast models use some type of uniform grid for their calculations. If we are going to routinely use observed data for any type of finite difference calculations, there is a need to transform or interpolate these irregularly spaced observations to the uniform grid without human intervention. This process is called objective analysis (OA). The following passage describes the method of the OA used in the supporting system.
The minimum value of grid spacing such as the JCOPE data or reanalysis data is a matter of 10km. Hereinafter, the mesh used for JCOPE data or reanalysis data is called as coarse mesh (CM), and the mesh finer than CM is called as fine mesh (FM).

1. First, the value on the CM at certain times is obtained by liner interpolation. It is called as "OBS."
2. Next, the number of the CM cell, which has the value of OBS, in which the coordinate of FM (x, y, z) is included is taken as (i, j, k).
3. Liner interpolation is used to determine the first estimate of the value at the point of fine mesh. The value at the certain coordinates of position, (x, y, z), is determined by liner interpolation as follows:

$$\begin{aligned}\phi(x,y,z) = {} & (1-\xi)(1-\eta)(1-\varsigma)\,\phi_{i-1,j-1,k-1} + (1-\xi)(1-\eta)\varsigma\,\phi_{i-1,j-1,k} \\ & + \xi\,(1-\eta)(1-\varsigma)\,\phi_{i,\ j-1,k-1} + \xi\,(1-\eta)\varsigma\,\phi_{i,\ j-1,k} \\ & + \xi\,\eta\,(1-\varsigma)\,\phi_{i,\ j,\ k-1} + \xi\,\eta\,\varsigma\,\phi_{i,\ j,\ k}\end{aligned} \quad (1)$$

Here,
$\phi_{i,j,k}$: the value of OBS, upper right of the coordinates of position (i, j, k)

$$\xi \equiv \frac{x - x_{i-1}}{x_i - x_{i-1}}, \qquad \eta \equiv \frac{y - y_{j-1}}{y_j - y_{j-1}}, \qquad \varsigma \equiv \frac{z - z_{k-1}}{z_k - z_{k-1}} \quad (2)$$

Three dimensional assimilation of wind/current field by MASCON model

The wind/current field data must satisfy the conservation of mass to calculate the advection and diffusion equation. The current data was calculated as the calculus of variations that sum of the change from initial value of interpolated current data would be minimum value. An approximated value was evaluated by solving the equation of the condition to restrict and to be minimum value by finite difference method. We describe a simple three dimensional assimilation method for wind/current field following MASCON method. [15, 16]
Suppose that we have a velocity field $\overline{\boldsymbol{v}}$ ($\phi(x, y, z)$, for example), which does not satisfy the continuity condition. We wish to create a new velocity field $\boldsymbol{v}$ which satisfies continuity and which is as close as possible to the original field $\overline{\boldsymbol{v}}$.
Mathematically, we can pose this problem as one of minimizing:

$$\tilde{R} = \frac{1}{2}\int_{\Omega} [\boldsymbol{v}(\boldsymbol{r}) - \overline{\boldsymbol{v}}(\boldsymbol{r})]^2\, d\Omega \quad (3)$$

where $\boldsymbol{r}$ is the position vector and Ω is the domain over which the velocity field is defined, subject to the continuity constraint

$$\boldsymbol{\nabla} \cdot \boldsymbol{v}(\boldsymbol{r}) = 0 \tag{4}$$

being satisfied everywhere in the field.

This is a standard type of problem of the calculus variations. A useful way of dealing with it is to introduce a Lagrange multiplier. The original problem (3) is replaced by the problem of minimizing:

$$R = \frac{1}{2}\int_{\Omega} [\boldsymbol{v}(\boldsymbol{r}) - \overline{\boldsymbol{v}}(\boldsymbol{r})]^2 \, d\Omega - \int_{\Omega} \lambda(\boldsymbol{r}) \boldsymbol{\nabla} \cdot \boldsymbol{v}(\boldsymbol{r}) \, d\Omega \tag{5}$$

where λ is the Lagrange multiplier. The inclusion of the Lagrange multiplier term does not affect the minimum value since the constraint (4) requires it to be zero.

Suppose that the function that minimizes the functional R is $\boldsymbol{v}^+$; $\boldsymbol{v}^+$ also satisfies (2):

$$R_{\min} = \frac{1}{2}\int_{\Omega} [\boldsymbol{v}^+(\boldsymbol{r}) - \overline{\boldsymbol{v}}(\boldsymbol{r})]^2 \, d\Omega \tag{6}$$

If $R_{\min}$ is a true minimum, then any deviation from $\boldsymbol{v}^+$ must produce a second-order change in R. Thus suppose that:

$$\boldsymbol{v} = \boldsymbol{v}^+ + \delta\boldsymbol{v} \tag{7}$$

where $\delta\boldsymbol{v}$ is small but arbitrary. When $\boldsymbol{v}$ is substituted into the expression (5), the result is $R_{\min} + \delta R$ where:

$$\delta R = \int_{\Omega} \delta\boldsymbol{v}(\boldsymbol{r}) \cdot [\boldsymbol{v}^+(\boldsymbol{r}) - \overline{\boldsymbol{v}}(\boldsymbol{r})] \, d\Omega - \int_{\Omega} \lambda(\boldsymbol{r}) \boldsymbol{\nabla} \cdot \delta\boldsymbol{v}(\boldsymbol{r}) \, d\Omega \tag{8}$$

We have dropped the term proportional to $(\delta\boldsymbol{v})^2$ as it is of second order. Now, integrating the last term by parts and applying Gauss's theorem, we obtain:

$$\delta R = \int_{\Omega} \delta\boldsymbol{v}(\boldsymbol{r}) \cdot [\boldsymbol{v}^+(\boldsymbol{r}) - \overline{\boldsymbol{v}}(\boldsymbol{r}) + \boldsymbol{\nabla}\lambda(\boldsymbol{r})] \, d\Omega + \int_{S} \lambda(\boldsymbol{r}) \delta\boldsymbol{v}(\boldsymbol{r}) \cdot \boldsymbol{n} \, dS \tag{9}$$

On the parts of the domain surface on which a boundary condition on $\boldsymbol{v}$ is given (walls, inflow), it is presumed that both $\boldsymbol{v}$ and $\boldsymbol{v}^+$ satisfy the given condition so $\delta\boldsymbol{v}$ is zero there. These portions of the boundaries make no contribution to the surface integral in (9) so no condition on λ is required on them; however, a condition will be developed below. On those parts of the boundary where other types of boundary conditions are given (symmetry planes, outflows) $\delta\boldsymbol{v}$ is not necessarily zero; to make the surface integral vanish, we need to required that $\lambda = 0$ on these portions of the boundary.

If δR is to vanish for arbitrary $\delta\boldsymbol{v}$, we must require that the volume integral in Eq. (9) also vanishes, i.e.:

$$\boldsymbol{v}^+(\boldsymbol{r}) - \overline{\boldsymbol{v}}(\boldsymbol{r}) + \boldsymbol{\nabla}\lambda(\boldsymbol{r}) = 0 \tag{10}$$

Finally, we recall that $\boldsymbol{v}^+(\boldsymbol{r})$ must satisfy the continuity equation (4). Taking the divergence of (10) and applying this condition, we find:

$$\nabla^2\lambda(\boldsymbol{r}) = \boldsymbol{\nabla} \cdot \overline{\boldsymbol{v}}(\boldsymbol{r}) \tag{11}$$

which is a Poisson equation for $\lambda(\boldsymbol{r})$. On those portions of the boundary on which boundary conditions are given on $\boldsymbol{v}$, $\boldsymbol{v}^+ = \overline{\boldsymbol{v}}$. Equation (10) shows that in this case $\boldsymbol{\nabla}\lambda(\boldsymbol{r}) = 0$ and we have a boundary condition on λ.

If (11) and the boundary conditions are satisfied, the velocity field will be divergence free. Once the Poisson equation in solved, the corrected velocity field is obtained from (10) written in the form:

$$\boldsymbol{v}^+(\boldsymbol{r}) = \overline{\boldsymbol{v}}(\boldsymbol{r}) - \boldsymbol{\nabla}\lambda(\boldsymbol{r}) \tag{12}$$

This shows that the Lagrange multiplier λ essentially plays the role of the pressure and again shows that, in incompressible flows, the function of the pressure is to allow continuity to be satisfied.

Dispersion of a radioactive material[17]

The turbulent velocity components of particles representing a passive tracer are derived from a first order Markov chain scheme under the following assumptions which are consistent with the second-order turbulence closure applied in the mesoscale meteorological model:

- Particles are assumed to take up the same distribution of velocities as the air;
- Turbulence is non-homogeneous in the horizontal;
- Turbulence is Gaussian: turbulent components of wind have normal distributions with zero mean values and variances $(\sigma_u^2, \sigma_v^2, \sigma_w^2)$ (the second order-closure scheme does not provide information on higher order moments);
- Particles are assumed to move independently (one-particle model), so the results are applicable only to ensemble-averaged diffusion.

The Markov chain scheme is defined by

$$\begin{cases} u'(t) = R_u u'(t-\Delta t) + (1-R_u^2) r_u \\ v'(t) = R_v v'(t-\Delta t) + (1-R_v^2) r_v \\ w'(t) = R_w w'(t-\Delta t) + (1-R_w^2) r_w \end{cases} \quad (13)$$

where,

(r_u, r_v, r_w) : random uncorrelated components

$(\sigma_u^2, \sigma_v^2, \sigma_w^2)$: variances of wind velocity components

(R_u, R_v, R_w) : Lagrangian autocorrelations of wind velocity components for lag time Δt assumed to be simple exponential functions:

$$\begin{cases} R_u(\Delta t) = \dfrac{\overline{u'(t)\cdot u'(t-\Delta t)}}{\sigma_u^2} = \exp\left(-\dfrac{\Delta t}{T_{Lu}}\right) \\ R_v(\Delta t) = \dfrac{\overline{v'(t)\cdot v'(t-\Delta t)}}{\sigma_v^2} = \exp\left(-\dfrac{\Delta t}{T_{Lv}}\right) \\ R_w(\Delta t) = \dfrac{\overline{w'(t)\cdot w'(t-\Delta t)}}{\sigma_w^2} = \exp\left(-\dfrac{\Delta t}{T_{Lw}}\right) \end{cases} \quad (14)$$

where,

(T_{Lu}, T_{Lv}, T_{Lw}) : Lagrangian integral time scales

When σ_w^2 is a function of height, the random component r_w of the vertical velocity w' must have nonzero mean value to prevent spurious accumulation of particles in regions of low turbulence:

$$\overline{r_u} = \overline{r_v} = 0, \qquad \overline{r_w} = \big(1 - R_w(\Delta t)\big) T_{Lw} \frac{\partial \sigma_w^2}{\partial z} \quad (15)$$

Distributions of r_u, r_v are Gaussian with zero mean values. The variances of r_u, r_v, r_w are equal to the variances of wind velocity components, $\sigma_u^2, \sigma_v^2, \sigma_w^2$ respectively. The random fluctuations are generated at each time step as:

$$r_u = \sigma_u \eta_u, \qquad r_v = \sigma_v \eta_v, \qquad r_w = \sigma_w \eta_w \quad (16)$$

η_i : random numbers picked up from a standard Gaussian distribution

Basic equation

The basic equation in the three-dimensional diffusion equation in consideration of nuclides decay and scavenging:

$$\frac{\partial C}{\partial t} + \boldsymbol{u}\cdot\boldsymbol{\nabla} C = \frac{\partial}{\partial x}\left(D_{\mathrm{h}} \frac{\partial C}{\partial x}\right) + \frac{\partial}{\partial y}\left(D_{\mathrm{h}} \frac{\partial C}{\partial y}\right) + \frac{\partial}{\partial z}\left(D_{\mathrm{v}} \frac{\partial C}{\partial z}\right) - \lambda C \quad (17)$$

C: Radionuclide concentration, t: Times, x, y, z: Geographical coordinates, $\boldsymbol{u}$: Advective velocity, $D_{\mathrm{h}}, D_{\mathrm{v}}$: Ocean diffusion coefficient and λ: radioactive decay constant. The diffusion

coefficient in the horizontal direction were assumed to be based on Richardson's law of 4/3 powers on the condition that the order of diffusion in the horizontal direction is tens of km (**Table 1**).

Table 1. Diffusion coefficient in the vertical direction of the ocean (cm^2/sec)

surface layer 0-100m	depths 1000m-	boundary layer on the sea bed
10-100	1-10	1-10

Estimation of concentration and doses

The supporting system outputs air concentration at the ground level, wet and dry depositions, air dose rate, gamma external dose and internal doses due to inhalation.

Dry and wet depositions

The dry and wet depositions are considered in the supporting system. The dry deposition can be expressed by

$$C_{\mathrm{dry}} = C_0 \exp\left(-\frac{V_{\mathrm{dep}} T_{\mathrm{fly}}}{z}\right) \quad (18)$$

C_{dry}: activity concentration at height z [Bq/m^3]

C_0: activity concentration at height z without depositions [Bq/m^3]

V_{dep}: dry deposition velocity [m/s] (summarized in **Table 2**)

T_{fly}: fright time of the particle [s]

Table 2. Deposition velocity (particle density: 1000kg/m^3)

Particle diameter [μm]	Diameter (average) [μm]	Deposition velocity [cm/s]
0.0 ～2.0	1.0	0.0029
2.1 ～5.0	3.5	0.036
5.1 ～10.0	7.5	0.16
10.1 ～20.0	15.0	0.65
20.1 ～40.0	30.0	2.61
40.1 ～	60.0	10.4
	Iodine	1.0

The wet deposition can be expressed by

$$C_{\mathrm{wet}} = C_0 \exp\left(-\Lambda T_{\mathrm{fly}}\right) \quad (19)$$

C_{wet}: activity concentration at height z [Bq/m^3]

C_0: activity concentration at height z without depositions [Bq/m^3]

T_{fly}: fright time of the particle [s]

Λ: washout coefficient [/s], $\Lambda = a \cdot I^b$. Here, coefficient a and b are shown in below:

	a	b
Iodine	8.0e-5	0.6
aerosol	1.2e-4	0.5

Air concentration

A Kernel Density Estimation (KDE) method is applied to prevent the statistical error. The KDE method is one of methods to estimate concentration from the distribution of particles. In this

method, a numerical function particles' mass is employed. In the supporting system, the distribution of each particles' mass is assumed to be the Gaussian. Thus, the concentration which is allotted to the evaluation point (x, y, z) from the unit-mass particle at the point (x_n, y_n, z_n) is expressed by

$$\chi(x,y,z) = \frac{1}{\left(\sqrt{2\pi}\right)^3}\frac{1}{\sigma_{x_n}\sigma_{y_n}\sigma_{z_n}}\exp\left\{-\frac{(x_n-x)^2}{2\sigma_{x_n}^2}\right\}\exp\left\{-\frac{(y_n-y)^2}{2\sigma_{y_n}^2}\right\} \cdot\left[\exp\left\{-\frac{(z_n-z)^2}{2\sigma_{z_n}^2}\right\}+\exp\left\{-\frac{(z_n{}'-z)^2}{2\sigma_{z_n}^2}\right\}\right] \quad (20)$$

where,
$\chi(x, y, z)$: the air concentration at the evaluation point (x, y, z)
$\sigma_{x_n}, \sigma_{y_n}, \sigma_{z_n}$: standard deviations of KDE [m]
Q_i: activity of particle *n* [Bq]
$z_n{}'$: height of the reflection particle [m]

Air dose rate and external dose to gamma-ray

The KDE method is also applied to the air dose rate calculation due to a radioactive cloud. The air dose rate D_i which is allotted to the evaluation point (x, y, z) from the unit-mass particle at the point (x_n, y_n, z_n) are pre-calculated. The equation D_i is

$$D_i = \iiint_{-\infty}^{+\infty} \frac{K_1 \mu_{\text{en}} E_\gamma \exp(-\mu r)}{4\pi r^2} B(E,r)\chi(x,y,z)dxdydz \quad (21)$$

where,
$\chi(x, y, z)$: the air concentration at the evaluation point (x, y, z)
K_1: dose conversion factor [dis m^3 Gy / MeV Bq hr]
E_γ: effective energy of gamma-ray [MeV/dis]

Internal dose due to inhalation

Internal doses D_{inh} due to inhalation are calculated by following equation,

$$D_{\text{inh}} = \chi(x,y,z) \cdot R \cdot D_f \quad (22)$$

here,
$\chi(x, y, z)$: air concentration of nuclide [Bq/m^3]
R: respiration rate [m^3/h]

	R[18]
child	0.31
adult	1.20

D_f: Dose conversion factor for effective dose equivalent [Sv/Bq]

	D_f[18]
^{131}I	1.6e-7
^{239}Pu	1.2e-4

In the outputs mentioned above, air concentration, deposition and air dose rate due to cloud-shine are calculated in every time step and accumulated during the output dump interval.

Release rate of nuclides from the package to the atmosphere

The decision of a release rate of nuclides from the package to the atmosphere was the very difficult problem. In the supporting system, we decided to use the release rate of nuclides to

atmosphere which derived from the risk study for spent fuel shipment.[19] Material release fractions to cask cavity is summarized in **Table 3**.

Table 3. Material release fractions to cask cavity[19]

Impact velocity [km/h] <drop height>	Cask Cavity Temperature (centigrade)	Release Mechanism	Particles	Ru	Cs	Gas (PWR)	Gas (BWR)
≦145 <83m>	Normal (160)	Damage to the cask containment due to drop impact	6.9E-06	4.8E-06	9.0E-07	4.9E-02	1.5E-01
	~350	Damage to the cask containment due to drop impact	6.9E-06	4.8E-06	3.7E-05	4.9E-02	1.5E-01
	~750	Damage to the cask containment due to drop impact and fire	1.2E-05	4.8E-06	2.0E-04	4.9E-02	1.5E-01
	>750	Damage to the cask containment due to drop impact and fire	2.4E-05	9.8E-06	2.5E-03	8.5E-01	8.4E-01
≦97 <37m>	Normal (160)	Damage to the cask containment due to drop impact	6.3E-08	2.7E-07	9.0E-10	2.4E-02	7.3E-02
	~350	Damage to the cask containment due to drop impact	6.3E-08	2.7E-07	3.7E-08	2.4E-02	7.3E-02
	~750	Damage to the cask containment due to drop impact and fire	3.1E-06	2.4E-06	7.8E-08	2.4E-02	7.3E-02
	>750	Damage to the cask containment due to drop impact and fire	1.2E-05	9.8E-06	2.5E-03	8.4E-01	8.4E-01
≦49 <9m>	>750	Damage to the cask containment due to fire	4.2E-06	9.8E-06	2.5E-03	8.4E-01	8.4E-01

EVALUATION RESULTS FOR SOME HYPOTHETICAL CONDITION USING THE SUPPORTING SYSTEM

Verification for atmospheric dispersion simulation

Activity concentration in the atmosphere was evaluated at the distance downwind in the case that accumulated loss of radioactive contents by the developed supporting system. The environmental condition is that wind velocity is 6 m/s, height of release point is 10 m, stability of atmosphere is most stable condition, “D” and the terrain is flat. Material release fraction to cask cavity is assumed to the accident which the impact velocity is less than 97 km/h and the cask cavity temperature is about 750 centigrade.

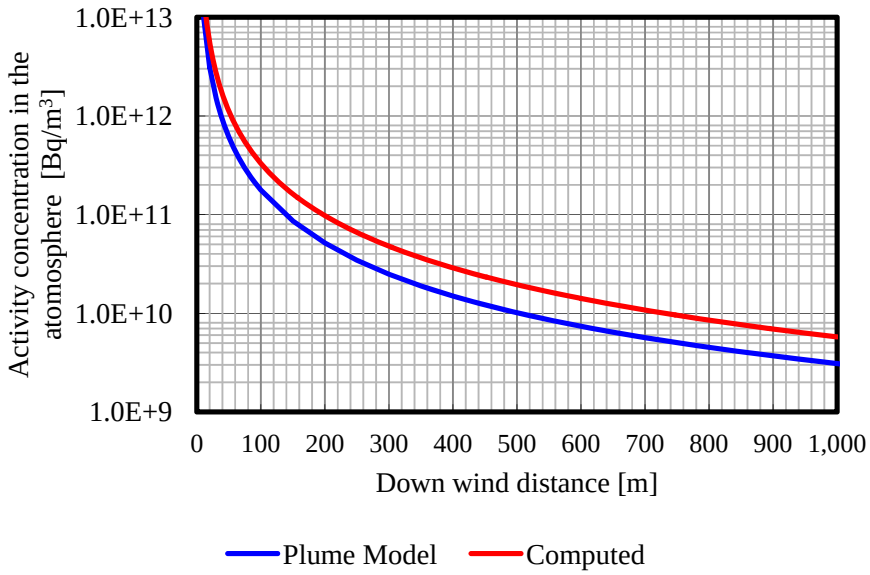

Figure 2. The results of atmospheric dispersion simulation

The results of atmospheric dispersion simulation are as **Figure 2**. For comparison, this figure contains the result of plume model. The result of the supporting system agrees well with the plume model.

Validation for dispersion of radionuclides in the marine environment

Nuclide concentration near shore was evaluated by using the supporting system. It assumed that the package for spent nuclear fuels is submerged on the seabed at the depth of 200m. In the present study, the barrier effect scenario that the presence of the package reduces the release rate of nuclides to the ocean was employed described in the literature.[20] The methods for determining the release of nuclides into the seawater by the barrier effect scenario are clearly described by *Tsumune et.al.*,[20] and are not repeated here (**Table 4**, **Table 5**).

Table 4. Hypothesis scenario of marine diffusion calculation [20]

Scenario of assessment	1. The package is submerged on the seabed at the depth of 200m. 2. After submergence, sealing function is lost by a functional disorder of O-ring immediately. 3. Seawater enters into the cavity of the package. 4. All fuel pellets exposes to the seawater. 5. Nuclides leach into the seawater in the cavity of the package. 6. The solution of nuclides is released to the ocean through the seal gap.
Release of nuclides into the seawater	The barrier effect scenario that the presence of the package reduces the release rate of nuclides to the ocean was employed.
Nuclides concentration	Nuclide concentration was evaluated calculating three-dimensional diffusion equation in consideration of nuclides decay and scavenging (nuclides removed from seawater by phenomena that nuclides absorb suspended materials in seawater and settle down the seabed).

Table 5. Release rate of Nuclides (Spent Fuel Package)[20]

Nuclides	Release Rate per Package (Bq/y)
Sr-90	2.80E+13
Y-90	2.80E+13
Sb-125	3.40E+10
Te-125m	1.40E+10
Cs-134	1.80E+11
Cs-137	4.00E+13
Ba-137m	3.70E+13
Pm-147	3.30E+11
Sm-151	6.00E+11
Eu-154	8.40E+11
Eu-155	2.40E+11
Pu-238	4.90E+10
Pu-241	1.80E+12
Am-241	2.70E+10
Cm-244	5.80E+11

The distribution of the nuclide concentration to be calculated in the ocean was evaluated. In the present study, we used the reanalysis data of JCOPE data. **Table 6** shows the maximum

concentration of nuclides in the surface layer which is the habitant of most of fishes ingested, 0-100m. In the literature 20, the advective velocity was assumed to be uniform regardless of depth direction and the velocity from north to south was assumed to be constant (12 cm/s). However, the calculated concentration in the supporting system is similar to that of literature 20. This fact indicates that the moving distance of radioactive material per year is within at most 50 km.

Table 6. Result of marine diffusion simulation

Depth	Calculated Concentration	Reference [20]
0 m	10^{-14}~10^{-15} Bq/m^3	10^{-14}~10^{-15} Bq/m^3
100 m	10^{-14}~10^{-15} Bq/m^3	

CONSIDERATION OF ISSUES CONCERNING DEPOSITION OF MATERIALS ON THE BED / RESUSPENSION FROM THE BED SEDIMENT

Radionuclides are fixed to suspended particles and the bed sediment. Radionuclides in the dissolved phase and suspended particles are transported by advection and diffusion processes. Suspended particles may be deposited on the bed and depending on the magnitude of the currents, the bed sediment to the suspended particle phase. At the same time, desorption of radionuclides from the bed and suspended particles occurs. Absorption is described by a kinetic coefficient k_1 and desorption by a coefficient k_2. All these processes are summarized in **Figure 3**, where a grid cell incorporating these processes is shown. In this model, two grain size fractions are considered in the bed sediment: only the small particles can be resuspended and incorporated into the water column as suspended matter. [21]

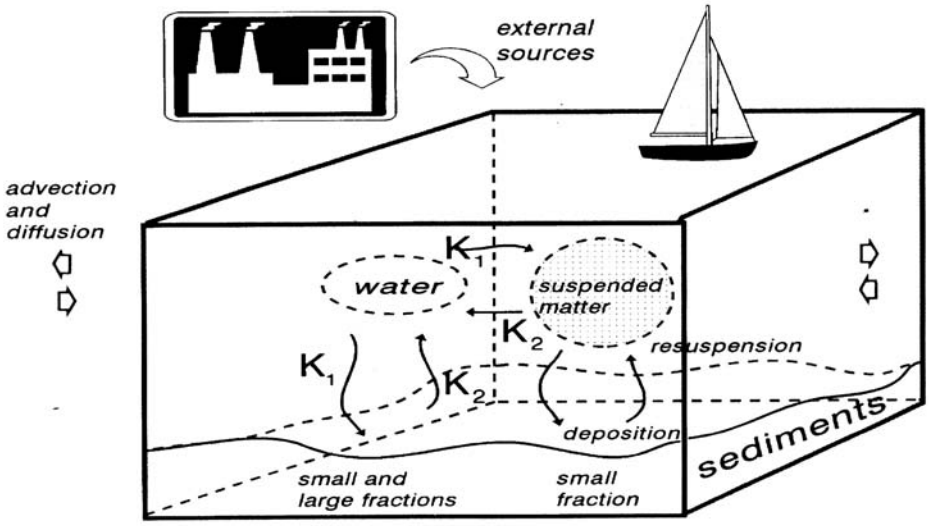

Figure 3. Grid cell showing processes affecting the dispersion of non conservative radionuclides [21]

The temporal evolution of specific activity in the dissolved phase

The equation that gives the temporal evolution of specific activity in the dissolved phase is C_{d}[Bq/m^3]:

$$\frac{\partial C_{\mathrm{d}}}{\partial t} + \boldsymbol{u}\cdot\boldsymbol{\nabla} C_{\mathrm{d}} = \frac{\partial}{\partial x}\left(D_{\mathrm{h}}\frac{\partial C_{\mathrm{d}}}{\partial x}\right) + \frac{\partial}{\partial y}\left(D_{\mathrm{h}}\frac{\partial C_{\mathrm{d}}}{\partial y}\right) + \frac{\partial}{\partial z}\left(D_{\mathrm{v}}\frac{\partial C_{\mathrm{d}}}{\partial z}\right) - (k_{11}+k_{12}+\lambda)C_{\mathrm{d}} + \mathrm{k}_2 m C_{\mathrm{s}} + \mathrm{k}_2 A_{\mathrm{s}} L \rho_{\mathrm{s}} f \phi \qquad (23)$$

where ,

$\boldsymbol{u}$: advective velocity [m/s]

$D_{\mathrm{h}}, D_{\mathrm{v}}$: Ocean diffusion coefficient
k_{11}: absorption rate from dissolved phase to suspended phase [/s]
k_{12}: absorption rate from dissolved phase to sediment phase [/s]
m: concentration of suspended material [kg/m^3]
C_{s}: specific activity in suspended matter [Bq/m^3]
k_2: desorption rate from suspended phase or sediment phase to dissolved phase [/s]
A_{s}: specific activity in the bed sediment [Bq/kg]
L: a mixing depth in the sediment (=0.1 m) [m]
ρ_{s}: sediment bulk density (=900 kg/m^3) [kg/m^3]
f: fraction of small particles
ϕ: correction factor

The temporal evolution of suspended sediment material

The equation that gives the temporal evolution of suspended sediment material is m[kg/m^3]:

$$\frac{\partial m}{\partial t} + \boldsymbol{u}\cdot\boldsymbol{\nabla} m = \frac{\partial}{\partial x}\left(D_{\mathrm{h}}\frac{\partial m}{\partial x}\right) + \frac{\partial}{\partial y}\left(D_{\mathrm{h}}\frac{\partial m}{\partial y}\right) + \frac{\partial}{\partial z}\left(D_{\mathrm{v}}\frac{\partial m}{\partial z}\right) + w_{\mathrm{s}}\frac{\partial m}{\partial z} + \left\{w_{\mathrm{s}} m\left(1-\frac{\tau_{\mathrm{b}}}{\tau_{\mathrm{cd}}}\right) - Ef\left(\frac{\tau_{\mathrm{b}}}{\tau_{\mathrm{ce}}}-1\right)\right\} \quad (24)$$

w_{s}: settling velocity for particle [m/s]

$$w_{\mathrm{s}} = \frac{\rho-\rho_w}{\rho_w}\frac{gD_i^2}{18\nu}$$

τ_{b}

τ_{cd}: critical deposition stress [N/m^2]
τ_{ce}: critical erosion stress [N/m^2]
E: erodability constant [kg/m^2 s]

The temporal evolution of radionuclide in the suspended phase

The equation that gives the temporal evolution of radionuclide in the suspended phase is C_{s}[Bq/m^3]:

$$\begin{aligned}\frac{\partial (mC_{\mathrm{s}})}{\partial t} + \boldsymbol{u}\cdot\boldsymbol{\nabla}(mC_{\mathrm{s}}) &= \frac{\partial}{\partial x}\left(D_{\mathrm{h}}\frac{\partial (mC_{\mathrm{s}})}{\partial x}\right) + \frac{\partial}{\partial y}\left(D_{\mathrm{h}}\frac{\partial (mC_{\mathrm{s}})}{\partial y}\right) \\ &+ \frac{\partial}{\partial z}\left(D_{\mathrm{v}}\frac{\partial (mC_{\mathrm{s}})}{\partial z}\right) + k_{11}C_{\mathrm{d}} + (\mathrm{k}_2+\lambda)mC_{\mathrm{s}} \\ &+ \left\{\frac{w_{\mathrm{s}}mC_{\mathrm{s}}}{\Delta z}\left(1-\frac{\tau_{\mathrm{b}}}{\tau_{\mathrm{cd}}}\right) - \frac{EfA_{\mathrm{s}}}{\Delta z}\left(\frac{\tau_{\mathrm{b}}}{\tau_{\mathrm{ce}}}-1\right)\right\}\end{aligned} \quad (25)$$

C_{s}: activity concentration of radionuclides in suspended matter and bottom sediments [Bq/m^3]
Δz: vertical grid size [m]

The temporal evolution of radionuclide in the sediment phase

The equation that gives the temporal evolution of radionuclide in the sediment phase is A_{s}[Bq/m^3]:

$$\frac{\partial A_{\mathrm{s}}}{\partial t} = k_{12}\frac{C_{\mathrm{d}}\Delta z}{L\rho_{\mathrm{s}}f} - \mathrm{k}_2 A_{\mathrm{s}}\phi - \lambda A_{\mathrm{s}} + \left\{\frac{w_{\mathrm{s}}mC_{\mathrm{s}}}{L\rho_{\mathrm{s}}f}\left(1-\frac{\tau_{\mathrm{b}}}{\tau_{\mathrm{cd}}}\right) - \frac{A_{\mathrm{s}}E}{L\rho_{\mathrm{s}}}\left(\frac{\tau_{\mathrm{b}}}{\tau_{\mathrm{ce}}}-1\right)\right\} \quad (26)$$

A_{s}: activity concentration in bed sediments [Bq/kg]
L: averaged mixing depth in bed sediment [m]
ρ_{s}: sediment bulk density [kg/m^3]

f: geometrical accessibility factor
k_{12}: absorption rate from dissolved phase to sediment phase [/s]

Distribution of ^{137}Cs in sediments near the Fukushima dai-ichi Nuclear Power Plant

The Fukushima Dai-ichi Nuclear Power Plant (1FNPP) operated by Tokyo Electric Power Corporation (TEPCO) was damaged by the great earthquake of magnitude 9.0 and the associated tsunami on 11 March, 2011. Nucear Emergency Response Headquarters, Government of Japan reported that a large amount of artificial radionuclides, including 1.5e16 Bq/L of ^{137}Cs, has been emitted to the atmosphere as a result of the damages. TEPCO also reported that 1484Bq/L of ^{137}Cs was detected at the south drain outlet on 21 March. Over 20,000Bq/L of ^{137}Cs was observed several times in front of 1FNPP. Ministry of Economy, Trade and Industry estimated that total amount of the radionuclides directly emitted in the early April. The monitoring report by Ministry of Education, Culture, Sports, Science and Technology (MEXT) mentioned that the maximum ^{137}Cs concentration at 30 km off the Fukushima coast was 186Bq/L on 15 April. This value is quite high as compared to the level of ^{137}Cs concentration observed before the Fukushima accident, 0 Bq/L. The temporal variation of ^{137}Cs concentration in front of 1FNPP suggests that most amounts of directly released ^{137}Cs were emitted in the initial period from March to the beginning of May 2011. We focused on the oceanic dispersion of ^{137}Cs. Possible physical processes around the 1FNPP is shown in **Figure 4**. [25]

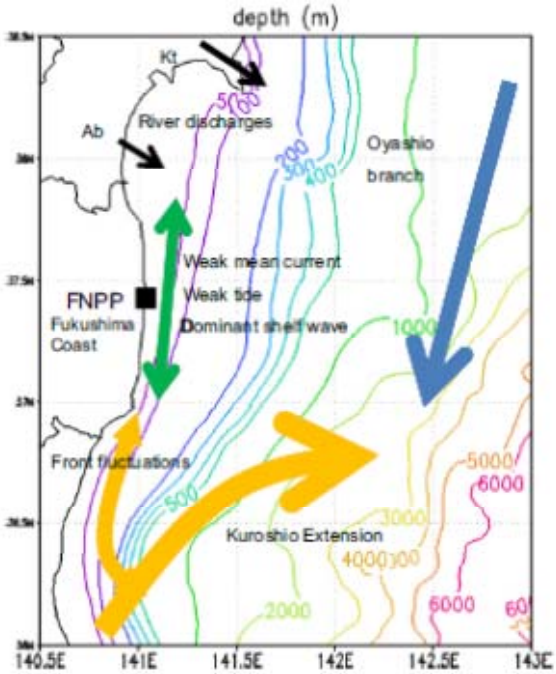

Figure 4. A schematic view outlining possible physical processes around the Fukushima Daiichi nuclear power plant [25] (Colored lines with numbers (in m) denote iso-depth contours.)

Observed data

TEPCO and MEXT have observed the concentrations of ^{131}I, ^{134}Cs and ^{137}Cs in marine soil near shore at several sites.[22, 23] We used observed data at the end of May 2012 and the end of March 2012 for the purpose of comparison to calculated result.

Estimated relase rates of ^{137}Cs calculated by using observed and simulation data

The methods for estimating release rate of ^{137}Cs are clearly described by *Tsumune et.al.*[13], and are not repeated here. **Figure 5** shows the estimated daily release rate of ^{137}Cs from 26 March to 31 May.

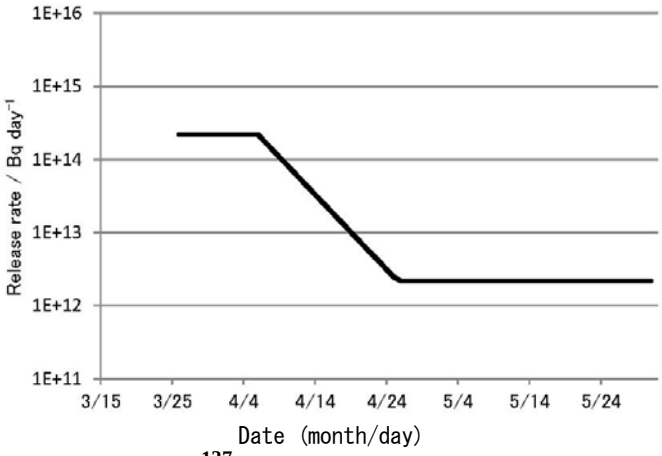

Figure 5. Estimated release rates of ^{137}Cs calculated by observed and simulation data. [13]

Computed distribution of ^{137}Cs in sediments

Figure 6 is computed distribution of ^{137}Cs at the end of March 2013 near the 1FNPP. **Figure 6(a)** indicates that ^{137}Cs released directly from the 1FNPP reactor was advected along the coast and transported to the open ocean by eddy: the released ^{137}Cs was advected to the Chiba and Miyagi coasts and then transported eastward by the Kuroshio Current. A schematic view of the current around the 1FNPP is shown in **Figure 4**.[25] **Figure 6(b)** indicates that ^{137}Cs in the suspended phase is affected by the current and eddy.

Figure 7 shows the computed distribution of ^{137}Cs in sediment near the 1FNPP. We compared the observed ^{137}Cs concentrations in sediments at some points. Computed distribution of ^{137}Cs in sediments is in good agreement with the end of May 2012 and the end of March 2013, which suggests that the model of deposition/resuspension described above is able to simulate the concentration of ^{137}Cs in sediments.

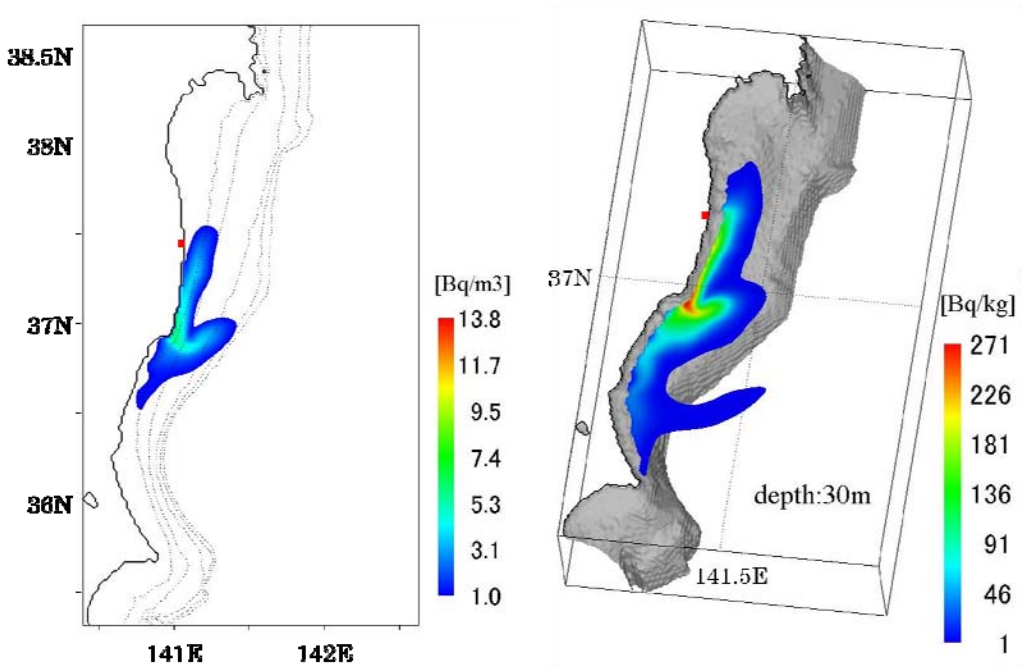

(a) Dissolved phase at sea surface **(b) Suspended phase at depth of 30 m**

Figure 6. Computed distribution of ^{137}Cs at the end of March 2013 near the Fukushima dai-ichi Nuclear Power Plant

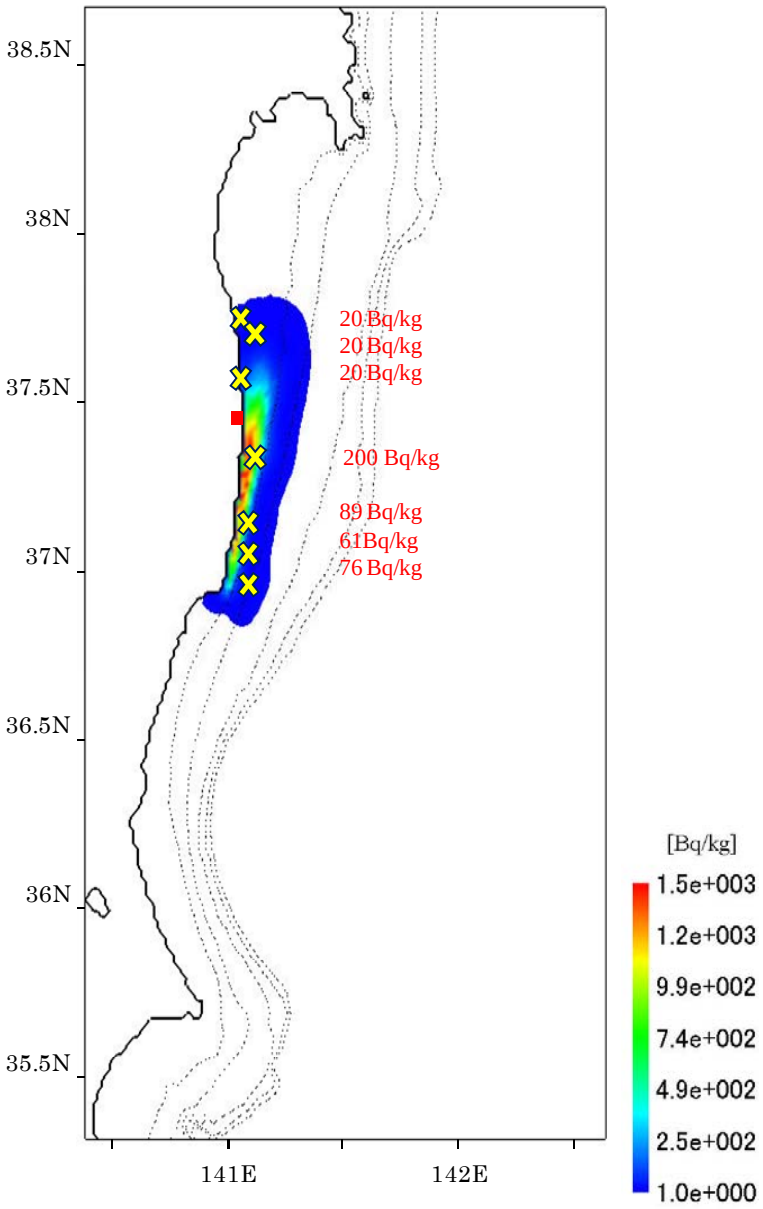

(a) End of May 2012

Figure 7. Computed distribution of ^{137}Cs in sediments [Bq/kg] on the seafloor near the Fukushima dai-ichi Nuclear Power Plant (Colored fonts denote measurement of the radioactivity at the point of yellowed on the end of May 2012. [22, 23])

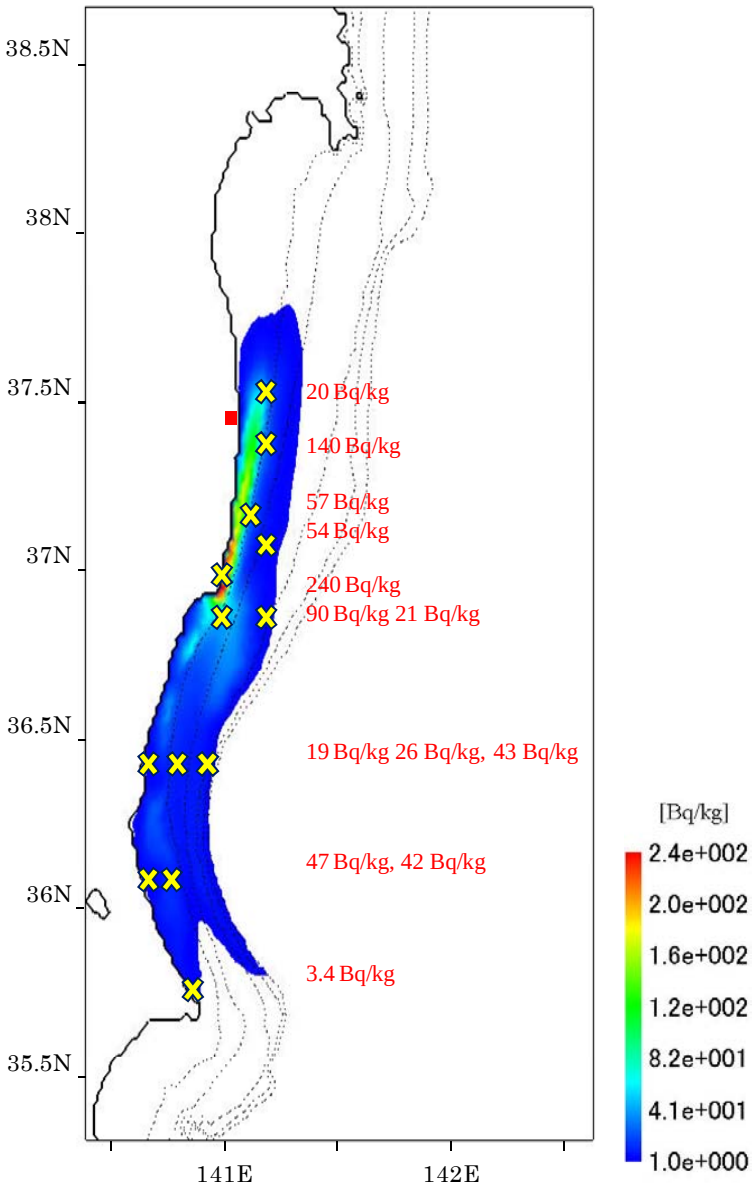

(b) End of March 2013

Figure 7. Computed distribution of ^{137}Cs in sediments [Bq/kg] on the seafloor near the Fukushima dai-ichi Nuclear Power Plant (Colored fonts denote measurement of the radioactivity at the point of yellowed on the January 2013. [22, 23])

CONCLUSION

The supporting system for emergency response to maritime transport accidents involving radioactive material was developed aiming support of accident response of Ministry of Land, Infrastructure and Transport, Japan, in case of the accident during maritime transport radioactive material. In the present study, basic functions of the supporting system were summarized and evaluation results applied to a hypothetical accident scenario were shown. The results indicated that the supporting system can carry out required simulation for emergency response very quickly with good enough accuracy.

ACKNOWLEDGMENTS

This study was conduct under a contract research “Development of accident assessment system for maritime transport of radioactive material” with Ministry of Land, Infrastructure and Transport, Japan.

REFERENCES

1. National Environmental Policy Act (NEPA) of 1969, Public Law 91-190, (1970).
2. U.S. NRC, “Final Environmental Statement on the Transportation of Radioactive Material by Air and Other Modes,” NUREG-0170, (1977).
3. Ruth F. Weiner, Douglas M. Osborn, Daniel Hinojosa, Terence J. Heames, Janelle Penisten, and David Orcutt, “RADCAT 2.3 User Guide,” SAND2006-6315, (2006).
4. International Atomic Energy Agency, “INTERTRAN A SYSTEM FOR ASSESSING THE IMPACT FROM TRANSPORTING RADIOACTIVE MATERIAL,” IAEA-TECDOC -287, (1983).
5. International Atomic Energy Agency, “GENERIC MODELS AND PARAMETERS FOR ASSESSING THE ENVIRONMENTAL TRANSFER OF RADIONUCLIDES FROM ROUTINE RELEASES,” Safety Series No.57, (1982).
6. F. A. Gifford, in Meteorology and Atomic Energy 1968 (D. H. Slade Ed.), USAEC Rep., TID-24, 190, (1968).
7. F. Pasquill, “Atmospheric Diffusion (2nd edition),” Ellis Horwood Ltd., Chichester, (1974).
8. T. Nagakura, Y. Maki and N. Tanaka, “Safety evaluation on transport of fuel at sea and test program on full scale cask in Japan”, PATRAM’78, Proceedings, (1978).
9. Science and technology Agency Japan (STA), Study to develop the system of transportation of plutonium -The case study for dose assessment-, (1992). (in Japanese)
10. N. Watabe, Y. Kohno, D. Tsumune, T. Saegusa and H. Ohnuma, “An Environmental Impact Assessment for Sea Transport of High Level Radioactive Waste,” *International Journal of Radioactive Materials Transport* 12/1995; **7**(2-3), pp.117-127, (1996).
11. H. Asano, M. Matsumoto and T. Saegusa, “An Environmental Impact Assessment for Sea Transport of Spent Fuel,” Proceedings of the 15th International Symposium on the Packaging and Transportation of Radioactive materials (PATRAM)1998, 961-965, (1998).
12. D. Tsumune, T. Saegusa, H. Suzuki, K. Maruyama, C. Ito and N. Watabe, “Estimated radiation dose from a MOX fuel shipping package that is hypothetically submerged into sea,” *International Journal of Radioactive Materials Transport* 12/1999; **11**(3), pp.239-253, (1999).
13. D. Tsumune, T. Tsubono, M. Aoyama and K. Hirose, “Distribution of oceanic ^{137}Cs from the Fukushima Daiichi Nuclear Power Plant simulated numerically by a regional ocean model,” *Journal of Environmental Radioactivity*, pp.1-9, (2011).
14. Y. Miyazawa and T. Yamagata, “2003: The JCOPE ocean forecast system,” First ARGO Science Workshop, November 12-14, 2003, Tokyo, Japan. http://www.jamstec.go.jp/frsgc/jcope/htdocs/topics/topics031112/poster031112.pdf
15. M. H. Dickerson, “MASCON – A Mass Consistent Atmospheric Flux Model for Regions with Complex Terrain,” *Journal of Applied Meteorology*, **17-3**, pp.241-253, (1978).
16. C. A. Sherman, “A Mass-Consistent Model for Wind Fields over Complex Terrain,” *Journal of Applied Meteorology*, **17-3**, pp.312-319, (1978).
17. R. L. Walko et al.,” HYPACT Hybrid PArticle and Concentration Transport Model version 1.2.0 User’s Guide,” Mission Research Corporation, (2001).
18. ICRP Publication71, “Age-dependent Doses to Members of the Public from Intake of Radionuclides: Part 4 Inhalation Dose Coefficients,” Annals of the ICRP Volume 25, 3-4, (1995).

19. U.S. Nuclear Regulatory Commission, “Reexamination of Spent. Fuel Shipment Risk Estimates: Main Report,” Sandia National Laboratories, NUREG/CR-6672, Vol. 1. SAND2000-0234, (2000).
20. D. Tsumune, H. Suzuki, T. Saegusa, N. Watabe, H. Asano, K. Maruyama and Y. Kinehara, “Dose Assessment for Public by Packages Shipping Radioactive Materials Hypothetically Sunk on the Continental Shelf”, pp. 91, Annex 3, IAEA-TECDOC-1231, (2001).
21. Raul Perianez, “Modelling the Dispersion of Radionuclides in the Marine Environment,” Springer Berlin Heidelberg New York, (2005).
22. MEXT: Ministry of Education, Culture, Sports, Science and Technology-Japan. Readings of Sea Area Monitoring at offshore of Miyagi, Fukushima, Ibaraki and Chiba Prefecture (marine soil).http://radioactivity.nsr.go.jp/en/contents/7000/6090/24/229_so_mfic_Sr_0322_14.pdf (published online March 22, 2013).
23. MEXT: Ministry of Education, Culture, Sports, Science and Technology-Japan. Distribution map of radioactivity concentration in the marine soil around coast of Fukushima Prefecture and TEPCO Fukushima Dai-ichi Nuclear Power Plant (Converted as dry soil). http://radio activity.nsr.go.jp/en/contents/7000/6177/24/20130322-02.pdf (published online March22, 2013).
24. N. ODANO and H. OKA, “Improvement of atmospheric and ocean dispersion model in supporting system for emergency response to maritime transport accident involving radioactive material,” Proceedings of the 15th International Symposium on the Packaging and Transportation of Radioactive materials (PATRAM) 2007, Oct. 21-26, (2007).
25. Y. Miyazawa, Y. Masumoto, S. M. Varlamov and T. Miyama, “Transport simulation of the radionuclide from the shelf to open ocean around Fukushima,” *Continental Shelf Research*, **50-51**, pp.16-29, (2012).